


Assessment of SPECT Image Reconstruction in Liver Scanning Using ^{99m}Tc /EDDA/HYNIC-TOC

Naeem Shareef Abdulhusein¹, Mohammad Reza Deevband^{1*} , Mohammad Ali Ghodsirad², Marziyeh Behmadi^{3,4}, Ghazal Mehri-Kakavand⁴

¹ Biomedical Engineering and Medical Physics Department, School of Medicine, Shahid Beheshti University of Medical Sciences, Tehran, Iran

² Nuclear Medicine Department, Shohada-e-Tajrish Hospital, Tehran, Iran

³ Cancer Research Center, Semnan University of Medical Sciences, Semnan, Iran

⁴ Department of Medical Physics, School of Medicine, Semnan University of Medical Sciences, Semnan, Iran

*Corresponding Author: Mohammad Reza Deevband
Email: mdeevband@sbmu.ac.ir

Received: 26 October 2021 / Accepted: 26 February 2023

Abstract

Purpose: Given that the Single Photon Emission Computed Tomography (SPECT) image quality is defined experimentally, developing a specialized scanning technique for each procedure is necessary to increase the diagnosis accuracy. This study aims to determine the optimal algorithm for liver scan reconstruction using ^{99m}Tc /SPECT.

Materials and Methods: The Filtered Back-Projection (FBP) reconstruction method was used in liver scanning using ^{99m}Tc -EDDA/HYNIC-TOC (Tektrotyd) for SPECT images of 30 patients which were acquired with a dual-head EvoExel detector system. Using different types of filters in SPECT imaging, various optimal results can be achieved in the processed images, such as artifact reduction, noise reduction, or signal enhancement and recovery. To evaluate the effect of different filters on image quality, Signal-to-Noise-Ratio (SNR), Contrast-to-Noise-Ratio (CNR), and contrast parameters were calculated.

Results: Applying filters enhanced contrast in the images in most cases as well as CNR and SNR. Metz (power = 2), Shepp-Logan (Cut-off frequency = 0.67) and Metz (power = 2) filters increase the CNR, contrast and SNR in images more than the other filters, respectively. The maximum improvement for CNR, contrast and SNR was from 0.62 to 2.35, 0.99 to 1.31, and 8.48 to 14.70, respectively.

Conclusion: Based on the results, the Hamming filter, due to providing high-quality images for visual analysis of liver SPECT, and the Butterworth filter, due to balancing the image quality and noise for quantitative analysis, are recommended.

Keywords: Single Photon Emission Computed Tomography Imaging; Filtering; Filter Design; Image Quality; Image Reconstruction.

1. Introduction

The normal function of the liver depends on the amount of hormones in the blood which is regulated by the endocrine glands and also mostly by the liver [1]. Now with the advent of advanced nuclear imaging techniques, it is feasible to evaluate directly liver function [2]. SPECT is enabled to evaluate the disease processes based on the cells and organs' functional and metabolic information [1, 2].

Filtered Back Projection (FBP) and iterative methods (such as Ordered Subset Expectation Maximization (OSEM)) are two methods that are utilized for the reconstruction of tomographic images [3]. The instrument improvement, development in computer-based image display, and new ^{99m}Tc labeled agents for visualizing biological events can enhance clinical efficiency in patient care and reduce diagnostic costs [4-6].

One of the important tasks in clinical SPECT imaging is noise reduction; therefore, different digital filters have been suggested [7]. Wiener, Butterworth, Parzen, Metz, Hamming, Ramp, and Shepp-Logan filters are commonly used in SPECT during reconstruction. The quality and accuracy of the image are greatly affected by applying these filters [3]. Different factors have an effect on the quality of the final tomographic image. Some of these factors are attenuation and scattering of photons, detection efficiency and spatial resolution of the imaging system, namely, the collimator and detector [3, 8]. Image filtering techniques are very important in medical imaging, especially in tomographic techniques, since they have a main effect on the image quality [9]. Noise reduction is performed through mathematical processes, including noise suppression, smoothing, edge enhancement, and recovery of resolution [9]. The physical parameters of the image including Contrast-to-Noise-Ratio (CNR), contrast, and Signal-to-Noise-Ratio (SNR) are the main criteria that are used for the evaluation of the performance of a filter [10]. According to the fact that the image quality of SPECT scans is established experimentally in the nuclear medicine departments [11, 12], designing a dedicated scanning method for ^{99m}Tc /SPECT is needed to improve the accuracy of disease diagnosis [13, 14].

Different authors investigated the effect of filtration on SPECT images. Lyra *et al.* in 2013 [15] evaluated different filters in 2D and 3D Cardiac SPECT Image

Processing. Mohseni *et al.* in 2015 [16] evaluated the effects of filtration on right ventricular function. Davidsson *et al.* in 2016 [17] investigated the effect of reconstruction algorithms on image quality in SPECT myocardial perfusion imaging. Sayed *et al.* in 2020 [7] compared the Low-Pass filters for SPECT Imaging. Park *et al.* in 2020 [10] used a median-modified wiener filter to improve the image quality of gamma camera images. Based on the literature review, there has been no study that investigated the quality optimization image with a combination of different filters and image reconstruction methods on liver scanning SPECT images.

This study aims to evaluate the effect of different filters on image quality, appraisal of quality criteria on image before and after the optimization and determination of the optimum algorithm for reconstruction in liver scanning using ^{99m}Tc for SPECT images.

2. Materials and Methods

This study was a retrospective study. The protocol and informed consent were considered by the research ethics committee of Shahid Beheshti University of Medical Sciences (Tehran, Iran) with a code number of IR.SB144.145P.REC.1400.443.

2.1. Data Collection and Techniques

In the Nuclear Medicine Department of Shohada-e-Tajrish Hospital (Tehran, Iran), SPECT studies were performed with a dual-head EvoExel detector system (Siemens Healthineers, Erlangen, Germany) using a Low-Energy, High-Resolution collimator (LEHR). Each experiment was performed 3-4 hours after intravenous injection of ^{99m}Tc -EDDA/HYNIC-TOC. A symmetric 15% wide energy window with a 140 keV center was used for the acquisition. As described in the literature [18, 19], each SPECT image was reconstructed using the FBP technique, which involves depth-dependent recovery of three-Dimensional (3D) resolution.

2.2. Sample Size Calculation

Based on the number of patients with the inclusion criteria, including demographic characteristics, sampling was performed by available sampling methods and it was estimated to be thirty patients.

The projections of SPECT images of 30 patients were received for both sexes (male and female). The projections were acquired in 20 minutes at 180 degrees using a parallel hole collimator with a photo-peak window of 129-150 keV and a scatter window of 108–129 keV.

2.3. Image Processing Toolbox (IPT)

In this study, MATLAB R2015b (MathWorks Inc., MA) software was used to design and apply various filters on the SPECT images. The Image Processing Toolbox (IPT) is used for image enhancement, image segmentation, noise reduction, filtering, image reconstruction, image restoration, geometric transformations, image registration, and 3D image processing operations. C/C++ code programs for use in computers and vision systems are supported by different functions in the IPT.

SPECT imaging was performed using the same detector system with twin-head cameras. A 128×128 matrix and a 60-step-and-shoot mode with 30-second step counting were utilized. Each head was confided to rotate through 1800 degrees for a total of 3600 SPECT acquisitions, starting from the left and right lateral locations, respectively.

2.4. Filter Designing

Different types of filters in SPECT imaging were used to achieve the various optimal results in the processed images, such as stellar artifact reduction, noise reduction, or signal enhancement and recovery. Generally, when the aim is to select the best filter for a particular image processing task, a trade-off is made between different effecting factors, including the noise reduction method, fine details suppression, contrast enhancement, and the spatial frequency pattern of the data on the image [3].

2.5. Image Analysis

The SPECT scans were processed using MATLAB software. One script code was written by the investigators to perform the FBP and Fourier transform on the images. Images were then analyzed in the same workstation.

After applying different filters to the images, Regions of Interest (ROIs) on the liver and background were determined. The mean and Standard Deviation (SD) of these two ROIs were calculated. Then, using the following equations, Signal-to-Noise-Ratio (SNR), Contrast-to-

Noise-Ratio (CNR) and contrast parameter were calculated using Equations 1, 2, and 3, respectively, to evaluate and compare the effect of different filters on the images [10].

$$SNR = \frac{ROI}{\sigma} \quad (1)$$

$$CNR = \frac{|ROI_L - ROI_B|}{\sqrt{\sigma_{Liver}^2 + \sigma_{Background}^2}} \quad (2)$$

$$Contrast = \frac{ROI_{Liver} - ROI_{Background}}{ROI_{Liver} + ROI_{Background}} \quad (3)$$

Where ROI is the constant in the region of interest, σ is the standard deviation of the value of ROI, ROI_{Liver} is the value from the region of interest in liver and $ROI_{Background}$ is the background value.

2.6. Calculation of Resolution

Gamma camera resolution is expressed by the full width at half maximum (FWHM) calculated from a point source profile. To calculate the resolution and the Modulation Transfer Function (MTF), the image of a point source was also taken.

To calculate FWHM, a Gaussian function fitted to the point-source profile was used and to calculate the resolution parameters the following relation was used for FWHM (Equation 4).

$$FWHM = 2\sqrt{-\ln(2)}\sigma \quad (4)$$

The Gaussian function fitted to the obtained profiles in the X-direction was written based on Equation 5:

$$f(x) = Ae^{-\left(\frac{x-\mu}{\sigma}\right)^2} \quad (5)$$

In the next step, different filters were designed and applied to the point source image. The results of the effect of different filters on the resolution were calculated and the obtained results are presented in the following sections.

2.7. Calculation of MTF

To calculate the MTF, the Point Spread Function (PSF) was obtained by considering the profile of the point source in the X- and Y-directions. The Fourier transform of this function was obtained and then the MTF of the system was calculated. To calculate these functions MATLAB software was used.

2.8. Image Quality Analysis

The SPECT scans were processed using MATLAB software by FBP and Fourier transform on the images. Different filters were applied to the images and a ROIs in the liver and the background were determined. The mean and standard deviation of these two ROIs were calculated and the image quality parameters were obtained to evaluate and compare the effect of different filters on the images. The effect of the filters on the image resolution of the point source was also investigated.

The other related results for image quality parameters such as CNR, contrast values, and SNR for different patients are extracted. To determine the optimal filter for qualitative (visual) and quantitative analysis of the SPECT images, each filter capacity for providing high contrast values and SNR were considered. To achieve this goal, the CNR, contrast values, and SNR values for each filter were determined. However, each filter type has a wide range of CNR, contrast, and SNR values based on the variable combination of filter settings that is utilized. To determine the filter's overall capability (in terms of CNR, contrast values, and SNR), the mean CNR, mean contrast values, and mean SNR were calculated. The optimal filter for qualitative and quantitative analysis was selected according to mean CNR, contrast values, and SNR.

3. Results

The point source image and its profile are shown in Figures 1 and 2. As it is clear, the point source image has a Gaussian profile.

The Gaussian function fitted to the obtained profiles in the X-direction is illustrated in Figure 3. The parameters

for the Gaussian function and the calculated resolution are listed in Table 1.

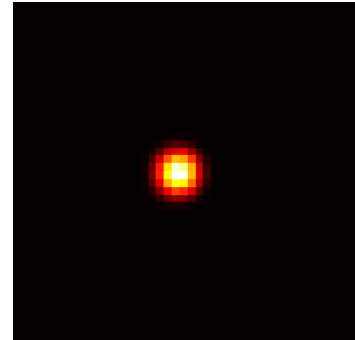


Figure 1. An image of a point source

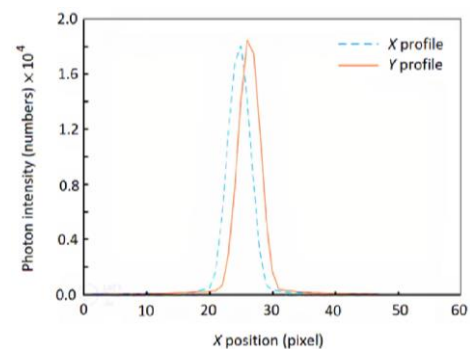


Figure 2. Profiles obtained by column-wise and row-wise summation of the point source image

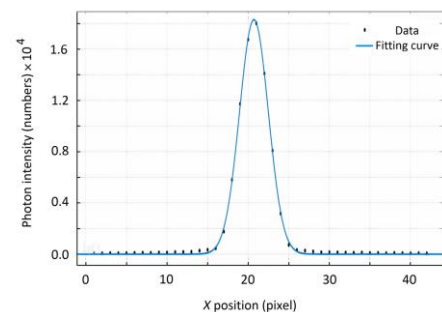


Figure 3. Gaussian function fitted to the profile in the X-direction

Table 1. Parameters of the Gaussian function and the resolution and fitting of the Gaussian function

Parameters		X-Direction	Y-Direction
	A	1.83×10^4	1.89×10^4
	μ	20.71	23.33
	σ	2.51	2.44
	FWHM (mm)	20.50	19.99
Goodness of fit	Sum of Squared Errors (SSE)	8.56×10^5	8.89×10^5
	Regression (R)-square	1.00	1.00
	Adjusted R-square	1.00	1.00
	Root-Mean-Square Error (RMSE)	148.10	142.20

The PSF profile to calculate the MTF in the X-directions is shown in Figure 4a. The magnitudes of the fast Fourier transform are presented in Figure 4b. The results of applying the filters to the images are visually shown in Figures 5 and 6, indicating the order and power of the filters.

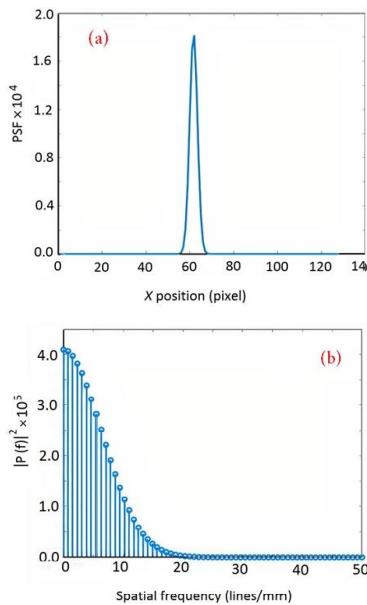


Figure 4. a) Profile extracted from the image of a point in X-direction. b) The magnitude of the fast Fourier transform (MTF) of the line profiles shown in (a)

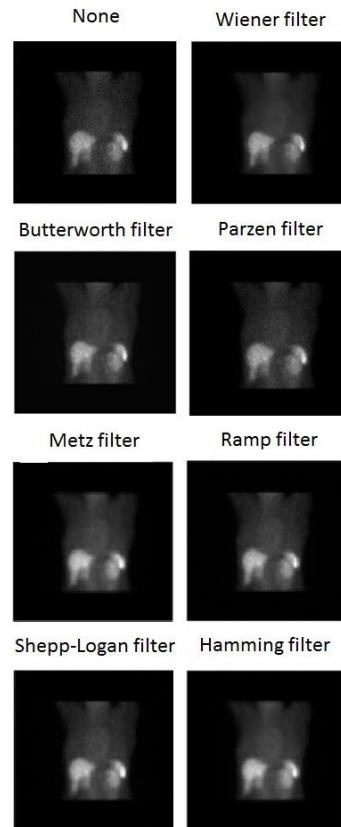


Figure 6. The effect of filters on the image quality, and the gray color map

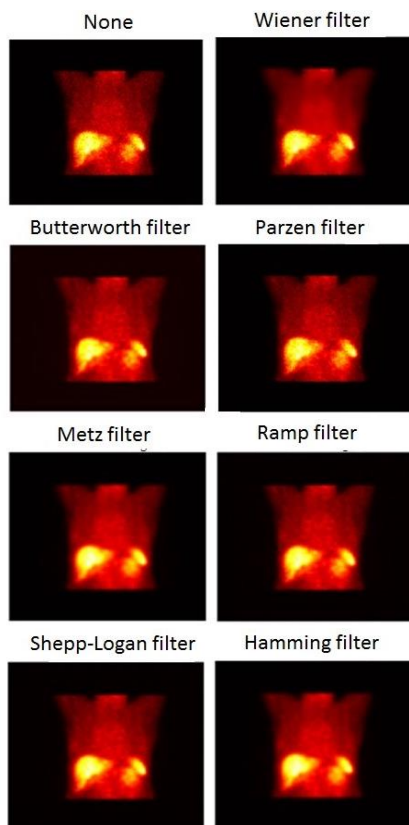


Figure 5. The effect of filters on the image quality saved the hot color map

Figure 7 shows the result of applying different filters on the image and the determination of ROIs in the liver and the background. In the following, Table 2 presented the results of the FWHM calculation after applying different filters.

The mean values of CNR, contrast values, and SNR and noise are presented in Table 3.

The effect of different filters on CNR, contrast values, and SNR are shown in Figure 8 (parts (a), (b), and (c)), respectively.

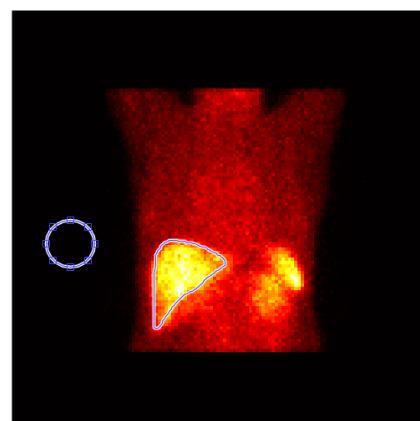


Figure 7. Selected ROIs in the background and the liver

Table 2. FWHM values in different filters

Filter type	Resolution (X-direction)	Resolution (Y-direction)
None	20.50	19.98
Wiener	20.62	20.03
Butterworth	20.57	20.02
Parzen	16.14	15.86
Metz	22.93	22.37
Ramp	21.51	20.98
Shepp-Logan	21.74	21.20
Hamming	22.80	22.24

4. Discussion

SPECT filters have a significant impact on the clinical quality of the images. Proper filter selection helps the physician in interpreting the data and making an accurate decision on diagnosis [20]. Digital filtering of SPECT images is accomplished by the selection of a window function from a list of one-dimension filters to be employed in the reconstruction, examining the generated image slices, and then repeating the process with a new window function if the results were unsatisfactory. The two-dimensional image restoration algorithms were considered in this study, and they are adapted spontaneously to the images being processed; therefore,

Table 3. Effect of different filters on the image quality parameters

Filter type	Mean CNR \pm SD	Mean contrast \pm SD	Mean SNR \pm SD
None	0.62 \pm 0.28	0.99 \pm 8.55 \times 10 ⁻⁵	8.48 \pm 1.14
Wiener	1.27 \pm 0.12	0.99 \pm 3.44 \times 10 ⁻⁴	11.22 \pm 1.61
Butterworth (power =2)	Cut-off frequency = 0.27	1.21 \pm 0.09	0.88 \pm 2.16 \times 10 ⁻⁴
	Cut-off frequency = 0.47	1.41 \pm 0.13	0.99 \pm 1.36 \times 10 ⁻⁴
	Cut-off frequency = 0.67	1.31 \pm 0.23	0.89 \pm 3.65 \times 10 ⁻⁴
Butterworth (power =4)	Cut-off frequency = 0.27	1.02 \pm 0.05	0.96 \pm 9.56 \times 10 ⁻⁴
	Cut-off frequency = 0.47	1.22 \pm 0.08	0.86 \pm 4.36 \times 10 ⁻⁴
	Cut-off frequency = 0.67	1.31 \pm 0.12	0.96 \pm 6.86 \times 10 ⁻⁴
Butterworth (power =6)	Cut-off frequency = 0.27	0.98 \pm 0.03	0.89 \pm 6.86 \times 10 ⁻⁴
	Cut-off frequency = 0.47	1.05 \pm 0.01	0.79 \pm 4.66 \times 10 ⁻⁴
	Cut-off frequency = 0.67	1.12 \pm 0.05	0.65 \pm 3.42 \times 10 ⁻⁴
Parzen	Cut-off frequency = 0.27	1.03 \pm 0.11	1.01 \pm 4.33 \times 10 ⁻⁴
	Cut-off frequency = 0.47	1.26 \pm 0.15	1.11 \pm 5.65 \times 10 ⁻⁴
	Cut-off frequency = 0.67	1.26 \pm 0.15	1.21 \pm 4.35 \times 10 ⁻⁴
Metz (power=2)	2.35 \pm 0.11	0.99 \pm 6.25 \times 10 ⁻⁴	14.70 \pm 1.22
Metz (power=4)	1.85 \pm 0.16	0.95 \pm 4.85 \times 10 ⁻⁴	11.30 \pm 0.92
Ramp	Cut-off frequency = 0.27	1.12 \pm 0.33	0.85 \pm 7.13 \times 10 ⁻⁵
	Cut-off frequency = 0.47	1.58 \pm 0.29	0.99 \pm 8.24 \times 10 ⁻⁵
	Cut-off frequency = 0.67	1.42 \pm 0.14	1.23 \pm 7.84 \times 10 ⁻⁵
Shepp-Logan	Cut-off frequency = 0.27	1.13 \pm 0.31	1.21 \pm 6.31 \times 10 ⁻⁴
	Cut-off frequency = 0.47	1.75 \pm 0.28	0.99 \pm 7.12 \times 10 ⁻⁴
	Cut-off frequency = 0.67	1.86 \pm 0.36	1.31 \pm 9.13 \times 10 ⁻⁴
Hamming	Cut-off frequency = 0.27	1.95 \pm 0.36	1.21 \pm 0.13
	Cut-off frequency = 0.47	2.29 \pm 0.22	0.99 \pm 0.01
	Cut-off frequency = 0.67	2.15 \pm 0.13	0.97 \pm 0.17

the need for repetitive reconstructions was eliminated. These filters have been demonstrated to significantly improve the image contrast and reduce noise levels compared to the Ramp filter reconstructions [3]. This image quality improvement was achieved by a slight increase in runtime when an array processor was utilized.

The data in Figure 8 demonstrate that various filters, in addition to changing the noise amplitude, alter the noise characteristics or its structure (also in Table 3). This occurs due to the fact that the filters modify not only the object's frequency components, but also the noise components [18]. Therefore, noise blobs are developed which may obstruct the identification of minor lesions. This fact should be considered whenever digital filtering is employed, and filters should be designed in a way that the risk of this effect is minimized.

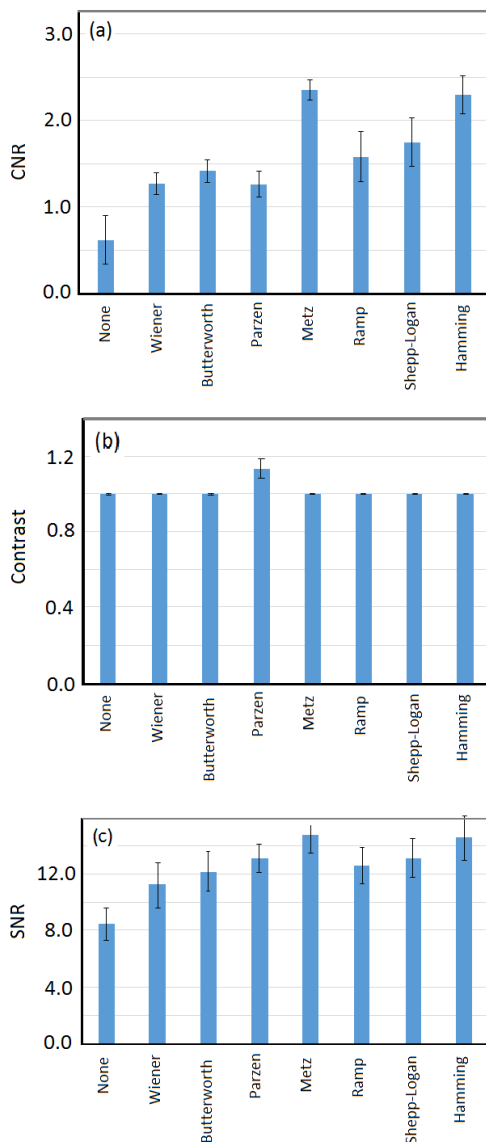


Figure 8. CNR (a), contrast (b) and SNR (c) values for different filters

As indicated in Table 3, the choice between pre- and post-reconstruction filtering of SPECT investigations is not totally evident. The investigators selected pre-reconstruction screening due to the following reasons: 1-Estimation of the noise power spectrum for a planar image is easier than a SPECT image. 2-With 2D pre-reconstruction filtering, a bigger statistical sample is employed to determine the value provided to the back-projector at each point. This is critical since SPECT imaging is photon-limited, and the extra information included in adjacent slice scans aids in noise reduction and contrast enhancement. 3-The blurring of images in SPECT may be overcome using a resolution recovery method [9, 19]. This preprocessing method beside the higher statistical sample size, enables the back-projector to receive more accurate input data and the results would improve the quality of SPECT images. The authors validated that for a given spatial location, the FWHM varies only about 1 mm in different directions for the images reconstructed using these filters. Post-reconstruction processing for resolution recovery has different advantages, one of them is less fluctuation for the spatial resolution (or MTF) across the tomographic slices compared to the planar images, as a function of distance from the collimator surface [21].

The authors believe that it is difficult to choose between Wiener and count-dependent Metz filtering. The Wiener filter has a good theoretical basis and adjusts the noise level of the image, the power spectrum of the object and the image blur (system MTF) [3, 16]. Although the count-dependent Metz filter, as implemented, responds exclusively to the changes in noise level, it has a speed advantage over the Wiener filter due to its simplicity [15]. In clinical images observation, it could not be seen any discernible change in the image quality between the use of either of these techniques to filter the SPECT images (Figure 8). This may be as a result of minor variances in object power spectra for clinical nuclear medicine images in comparison with the variation produced by various total counts, or it may be due to the optimization of both filters with minimization of the Mean Squared Error (MSE).

This study used more filters related to the other literature [7, 10, 15-17]. Sayed *et al.* in 2020 [7] reported that the Butterworth filter provided superior results than the Hamming filter. Lyra *et al.* in 2014 [15] indicate that the Butterworth filters for both 3D and 4D cardiac SPECT have the best results relative to Hamming and

Parzen filters. The other literature results are in disagreement with the authors' outcomes in this study which may be due to the organ and the condition of imaging.

The limitations of this study were as follows: The optimal filter may be different based on the machine and the organ. On the other hand, the size of the patient's body was not considered in this study. It would be a good idea to investigate the other organs, the filter type, and image quality based on the Body Mass Index (BMI) and different machines in the next studies.

5. Conclusion

Based on the results of this study, the Hamming filter is recommended for visual analysis of liver SPECT images due to its capacity for providing high-quality images. Instead, for quantitative analysis, the Butterworth filter is recommended due to the ability of this filter for providing a balance between the quality and noise for the SPECT images.

References

- 1- Genes SG. "Role of the liver in hormone metabolism and in the regulation of their content in the blood." *Arkh Patol*; 39(6): 74-80, (1977).
- 2- Espersen C, Borgwardt L, Larsen PN, Andersen TB, Stenholt L, Petersen LJ. "Nuclear imaging methods for the prediction of postoperative morbidity and mortality in patients undergoing localized, liver-directed treatments: a systematic review." *EJNMMI Res*; 10(1): 101, (2020).
- 3- Lyra M, Ploussi A. "Filtering in SPECT Image Reconstruction." *Int J Biomed Imaging 2011*; 693795, (2011).
- 4- Gullberg GT, Reutter BW, Sitek A, Maltz JS, Budinger TF. "Dynamic single photon emission computed tomography-basic principles and cardiac applications." *Phys Med Biol*; 55(20): 111-91, (2010).
- 5- Ljungberg M, Pretorius PH. "SPECT/CT: an update on technological developments and clinical applications." *Br J Radiol*; 91(1081): 20160402, (2018).
- 6- Velikyan I. "Prospective of ⁶⁸Ga-radiopharmaceutical development." *Theranostics*; 4(1): 47-80, (2013).
- 7- Sayed IS, Ismail SS. Comparison of Low-Pass Filters for SPECT Imaging. *Int J Biomed Imaging*; 2020: 9239753, (2020).
- 8- Frey EC, Humm JL, Ljungberg M. "Accuracy and precision of radioactivity quantification in nuclear medicine images." *Semin Nucl Med*; 42(3): 208-18, (2012).
- 9- Saib DMA, Azman NZN, Said MA, Aseri MIM, Almarri HM, Ramli RM. "Evaluation of butterworth post-filtering effects on contrast and signal noise to ratio values for SPECT images reconstruction." *Radiat Phys Chem*; 192: 109932, (2022).
- 10- Park CR, Kang S-H, Lee Y. "Median modified wiener filter for improving the image quality of gamma camera images." *Nucl Eng Technol*; 52(10): 2328-33, (2020).
- 11- Buvat I, Frey E, Green A, Ljungberg M. "IAEA human health report number 9. Quantitative nuclear medicine imaging: concepts, requirements and methods.", IAEA, Vienna, (2014).
- 12- Dorbala S, Ananthasubramaniam K, Armstrong IS, Chareonthaitawee P, DePuey EG, Einstein AJ, et al. "Single Photon Emission Computed Tomography (SPECT) Myocardial Perfusion Imaging Guidelines: Instrumentation, Acquisition, Processing, and Interpretation." *J Nucl Cardiol*; 25(5): 1784-846, (2018).
- 13- Al Moudi M, Sun Z-H. "Diagnostic value of 18F-FDG PET in the assessment of myocardial viability in coronary artery disease: A comparative study with ^{99m}Tc SPECT and echocardiography." *J Geriatr Cardiol*; 11(3): 229-236, (2014).
- 14- Zeintl J, Vija AH, Yahil A, Hornegger J, Kuwert T. "Quantitative accuracy of clinical ^{99m}Tc SPECT/CT using ordered-subset expectation maximization with 3-dimensional resolution recovery, attenuation, and scatter correction." *J Nucl Med*; 51(6): 921-8, (2010).
- 15- Lyra M, Ploussi A, Rouchota M, Synefia S. "Filters in 2D and 3D cardiac SPECT image processing." *Cardiol Res Pract 2014*; (2014).
- 16- Mohseni S, Kamali-Asl A, Bitarafan-Rajabi A, Entezarmahdi SM, Shahpouri Z, Yaghoobi N. "Effects of filtration on right ventricular function by the gated blood pool SPECT." *Ann Nucl Med*; 29(4): 384-90, (2015).
- 17- Davidsson A, Olsson E, Engvall J, Gustafsson A. "Influence of reconstruction algorithms on image quality in SPECT myocardial perfusion imaging." *Clin Physiol Funct Imaging*; 37(6): 655-62, (2017).
- 18- Choi MS, Kang HG. "Transient noise reduction in speech signal with a modified long-term predictor." *EURASIP J Adv Signal Process*; 2011(1): 141, (2011).
- 19- King MA, Schwinger RB, Doherty PW, Penney BC. "Two-dimensional filtering of SPECT images using the Metz and Wiener filters." *J Nucl Med*; 25(11): 1234-40, (1984).
- 20- Pandey A, Pant G, Malhotra A. "Standardization of SPECT filter parameters." *Indian J Nucl Med*; 19(2): 30-5, (2004).
- 21- Shahbazi-Gahrouei D, Arabpour A, Kermani S, Rastgoo F. "Assessment of gated single photon emission computerized tomography cardiac wall motion by using different reconstruction methods and filters in comparison with quantitative coronary angiography." *J Med Sci*; 8(4): 342-9, (2008).